X-ray photoemission spectroscopy studies of Sn-doped indium-oxide films[a)]

John C. C. Fan and John B. Goodenough[b)]

Lincoln Laboratory, Massachusetts Institute of Technology, Lexington, Massachusetts 02173
(Received 9 February 1977; accepted for publication 18 March 1977)

The In and Sn $3d_{3/2}$ and $3d_{5/2}$ ESCA peaks and the oxygen $1s$ peak of Sn-doped In_2O_3 films were compared with those for In_2O_3 films and In_2O_3, SnO, SnO_2, and Sn_3O_4 powders. Comparison of as-grown with sanded surfaces revealed Sn-rich surface layers in those films having good optical and transport properties. These experimental findings are interpreted with a schematic energy-band model and the assumption that film darkening in Sn-doped In_2O_3 films is caused by the formation and growth of an Sn_3O_4-like second phase in the bulk. Suppression of this phase could be accomplished by higher substrate temperatures, which permit equilibrium conditions to be attained: Sn-rich phases appear to migrate to the film surface, and the tin disproportionates to Sn^{2+} and Sn^{4+} ions.

PACS numbers: 79.60.Eq, 73.60.−n, 68.60.+q, 82.80.Pv

I. INTRODUCTION

Sn-doped In_2O_3 films are conducting and highly transparent to visible radiation,[1,2] which makes them useful for a variety of applications. We have been developing them for heat mirrors for solar collectors and for electrodes for solar cells.[1,3] The optical and electrical properties of these films are found to be sensitive to preparation conditions. In order to better understand the mechanisms responsible for the properties of these films, we have performed x-ray photoemission studies. From the results of these and other studies, we propose a band model to account for the known data on these films.

Boswell and Waghorne[4] reported x-ray photoemission experiments on films prepared from In_2O_3-20% SnO_2 mixed-powder targets. Their films were sputtered onto unheated substrates at low power density, and our results, as well as theirs, indicate that at low substrate temperatures Sn-doped In_2O_3 films probably contain Sn_3O_4 as a second phase. Since the optical and electrical properties of their films were not reported, meaningful comparison of their results with ours is not possible.

II. EXPERIMENTAL PROCEDURE

Sn-doped In_2O_3 films were deposited on 7059 glass substrates by rf sputtering from a 5-in.-diam hot-pressed target of In_2O_3 containing 9 mol% SnO_2.[1] Typical sputtering conditions were as follows: base pressure of about 10^{-6} Torr, a target-to-substrate distance of 5.7 cm, an argon pressure of 10^{-2} Torr, an argon flow rate of 0.5 cm^3/min, and presputtering for 15 min followed by deposition at the same power level. Film thicknesses were generally between 300 and 5000 Å. In_2O_3 and SnO_2 films were deposited by similar procedures using hot-pressed targets of In_2O_3 and SnO_2 (at a sputtering power of 550 W). Our x-ray photoemission studies (ESCA) were done in a McPherson ESCA (Model 36) apparatus.

The McPherson apparatus operates at a vacuum of better than 1×10^{-8} Torr and the specimens were irradiated with a MgK_α x-ray energy of 1254 eV. Chemical binding energies were obtained by subtracting the kinetic energies of the photoelectrons from this incident energy. Experimental uncertainties in the binding-energy determinations are about ±0.10 eV. In_2O_3 powder and films of SnO_2, In_2O_3, and Sn-doped In_2O_3 are sufficiently conducting that no charging effects were observed. However, some charging effects were noted for SnO, SnO_2, and Sn_3O_4 powders, and the position of the carbon $1s$ peak was taken as a standard (binding energy = 285.0 eV) to compensate for any charge-induced shifts. Most film measurements were done on as-grown surfaces, but a few were also done on films that were subsequently sanded in dry-N_2 gas with either SiC or Al_2O_3 sanding paper. Sanding rather than argon-ion sputtering was used to remove the as-grown surface because of the differential sputtering effects reported for this material system.[1] After sanding, some films exhibited slight charging effects that were corrected for by referral to the position of the carbon $1s$ peak. No Si or Al ESCA peaks were observed on sanded surfaces, indicating that no SiC or Al_2O_3 was deposited on the surface during sanding.

III. EXPERIMENTAL RESULTS

A. In $3d_{3/2}$ and $3d_{5/2}$ peaks

Figure 1 shows the ESCA data for In_2O_3 powder, an In_2O_3 film, and a Sn-doped In_2O_3 film before and after sanding. ESCA results of all the other samples were similar. (Because of different scaling factors used for the samples, the heights of ESCA peaks for this figure and all the following figures do not represent the actual intensities. When area ratios were taken, correct scaling factors were taken into account.) Significantly, the observed binding energies of the In $3d_{3/2}$ and In $3d_{5/2}$ levels are essentially the same, 444.5 and 452.1 eV, respectively, for all samples and agree with the values reported in the literature.[4] From this observation we conclude that the experimental system is stable, any charging effects are well eliminated, and the In peaks in all our samples are from ions with the formal valence state In^{3+}.

[a)]Work sponsored by the Department of the Air Force.
[b)]Present address: Inorganic Chemistry Laboratory, Oxford University, Oxford, England.

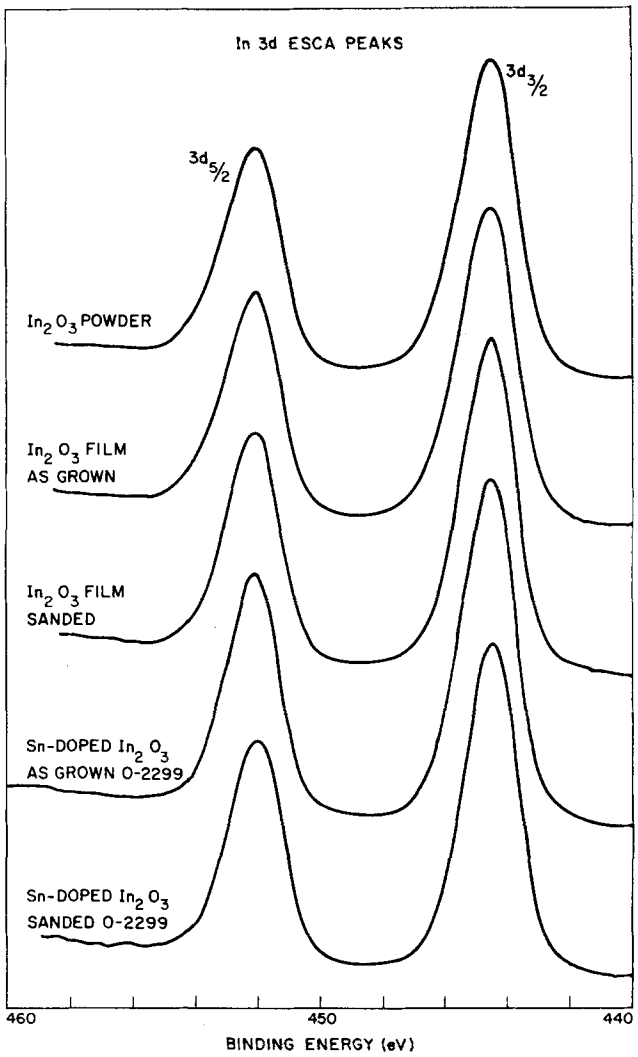

FIG. 1. In $3d_{3/2}$ and $3d_{5/2}$ ESCA peaks for In_2O_3 powder, an In_2O_3 film, and an Sn-doped In_2O_3 film before and after sanding.

B. Sn $3d_{3/2}$ and $3d_{5/2}$ peaks

The Sn $3d_{3/2}$ and $3d_{5/2}$ peaks from SnO_2, SnO, and Sn_3O_4 vary in position, as can be seen from Fig. 2. The same peaks from metallic Sn were found to be at 484.9 and 493.3 eV, respectively.

1. SnO_2

The Sn $3d_{3/2}$ and $3d_{5/2}$ peaks from SnO_2 powder and a SnO_2 film have essentially the same shapes and positions, and the measured peak positions 486.7 and 495.2 eV, respectively, correspond well with published values.[5] The symmetrical peaks are found to be Gaussian; a Lorentzian distribution function fits poorly.

2. SnO

The Sn $3d_{3/2}$ and $3d_{5/2}$ peaks from SnO powder are at 487.2 and 495.7 eV, respectively, indicating the unusual situation of a higher binding energy at ions of lower formal valence state, i.e., Sn^{2+} versus Sn^{4+}. This finding also corresponds well with published results.[5] As found for SnO_2, the Sn $3d_{3/2}$ and $3d_{5/2}$ peaks are well fit by Gaussian distribution functions.

3. Sn_3O_4

Whereas the SnO_2 and SnO powders were stoichiometric and single phase, x-ray powder diffraction revealed a few percent SnO_2 in the Sn_3O_4 gray powders received from Cerac, Inc., Wisc. Stoichiometric Sn_3O_4 powders are difficult to obtain. The Sn $3d_{3/2}$ and $3d_{5/2}$ peaks were found at 486.6 and 495.1 eV, only slightly less than those for SnO_2, and the Sn ESCA peaks are similarly Gaussian.

4. In_2O_3 - 5 mol% SnO_2 and - 5 mol% SnO powder

Figure 3 shows the Sn $3d_{3/2}$ and $3d_{5/2}$ peaks obtained from In_2O_3 powder mixed with 5 mol% SnO_2 and 5 mol% SnO. The composite structure of each peak is due to the superposition of SnO_2 and SnO peaks at different positions. Figure 4 shows the observed Sn $3d_{3/2}$ peak of the mixed powder and its resolution into Sn $3d_{3/2}$ peaks from SnO and SnO_2 powders; a similar resolution could also be made for the Sn $3d_{5/2}$ peak of the mixed powder. The resolution procedure used Gaussian functions with the positions and linewidths of the Sn 3d peaks of SnO and SnO_2; only the intensities of the peaks were variable. Since SnO and SnO_2 are equally mixed into In_2O_3 in the mixed powder, the 40/60 ratio for the relative intensities should approximate the relative sensitivities of the Sn $3d_{3/2}$ peaks of SnO and SnO_2.

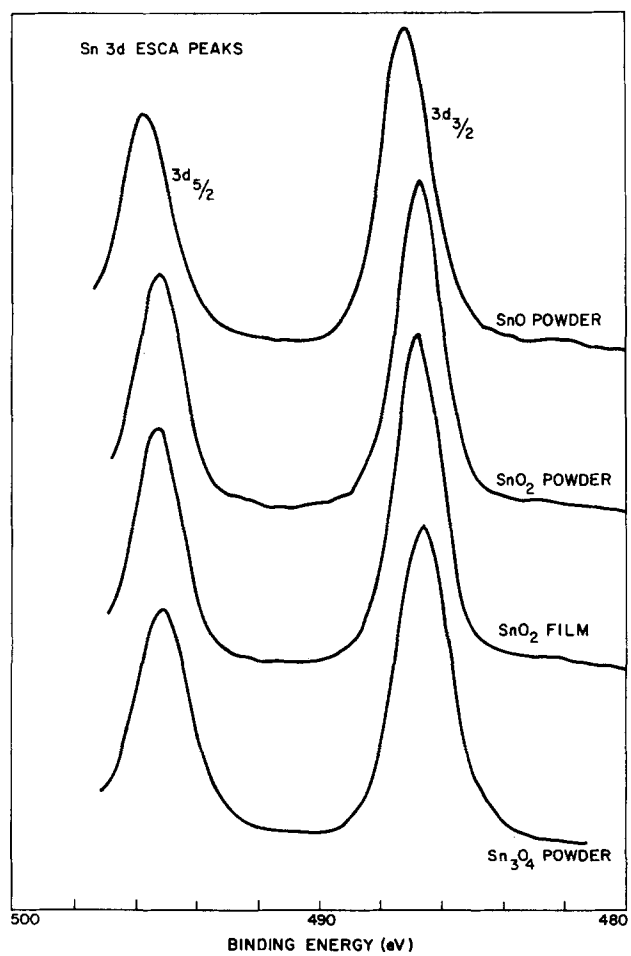

FIG. 2. Sn $3d_{3/2}$ and $3d_{5/2}$ ESCA peaks for SnO_2, SnO, and Sn_3O_4.

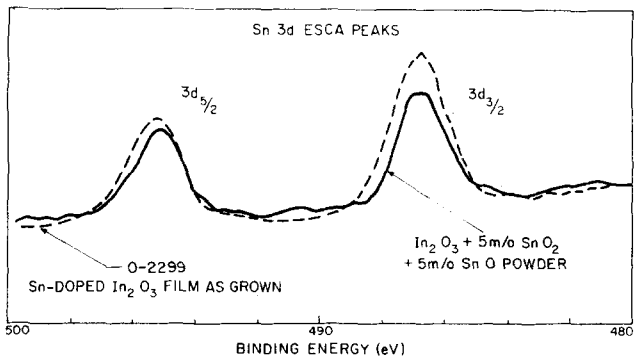

FIG. 3. Sn $3d_{3/2}$ and $3d_{5/2}$ ESCA peaks for In_2O_3 powder mixed with 5 mol% SnO_2 and 5 mol% SnO powders. Also included are Sn $3d_{3/2}$ and $3d_{5/2}$ peaks for an Sn-doped In_2O_3 film (0-2299), showing features similar to those of the mixed powder.

5. Films obtained from a 5-in. diam target of In_2O_3 - 9 mol% SnO_2

Figures 5 and 6 show the ESCA peaks for Sn $3d_{3/2}$ and $3d_{5/2}$ from films deposited on Corning 7059 glass from a 5-in-diam target of In_2O_3-9 mol% SnO_2 with sputtering powers of 100, 550, and 600 W, respectively. A detailed description of similar films prepared under these conditions has been published elsewhere.[1]

The 2-μm-thick 100-W film 0-1974 had a visible transmission of less than 20% and a room-temperature resistivity of 10^{-3} Ω cm (n-type conductivity). X-ray diffraction studies showed, in addition to In_2O_3 peaks, the presence of small Sn_3O_4 peaks.[1] (Another sample, prepared under similar conditions, had a room-temperature resistivity of about 2×10^{-3} Ω cm and a visible transmission of about 50%. Possibly because it was only 0.5 μm thick, no x-ray Sn_3O_4 peaks were observed.) From the as-grown surface, the Sn $3d_{3/2}$ and $3d_{5/2}$ positions (486.6 and 495.1 eV) were the same as those from Sn_3O_4 powder. There is some asymmetry of the peaks, indicating that multiple components may be present (as shown in Fig. 5). After sanding, the ESCA peaks were shifted significantly to lower binding energies, 486.3 and 494.7 eV. The Sn/In ratio, as calculated from the ratio of integrated areas under the Sn $3d_{3/2}$ and In $3d_{3/2}$ peaks, respectively, was essentially unchanged on going from the as-grown surface into the film; the Sn $3d_{3/2}$/In $3d_{3/2}$ ratios were 0.055 and 0.052 before and after sanding. Similar ESCA results were obtained on another sample prepared in the same deposition run.

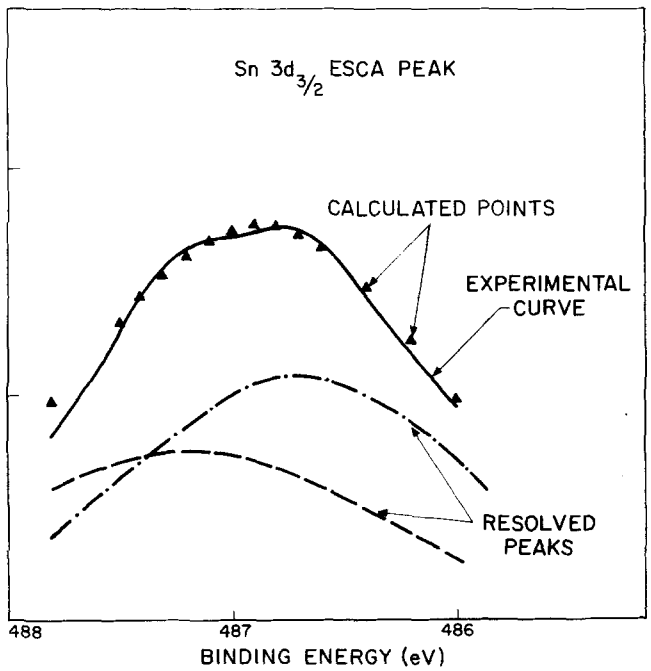

FIG. 4. Sn $3d_{3/2}$ peak of the mixed powder (shown in Fig. 3) resolved into two peaks. The calculated points represented the superposition of the two resolved peaks.

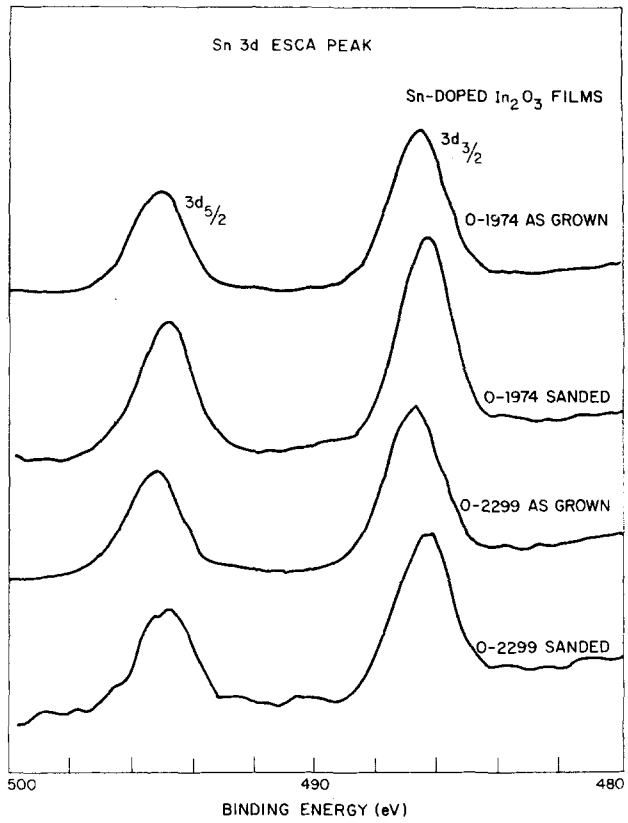

FIG. 5. Sn $3d_{3/2}$ and $3d_{5/2}$ ESCA peaks for Sn-doped In_2O_3 films (0-1974 and 0-2299) before and after sanding.

The 0.5-μm-thick 550-W film 0-2299, on the other hand, had a visible transmission of over 85% and a room-temperature n-type resistivity $\rho \approx 2.6\times10^{-4}$ Ω cm. X-ray diffraction showed only the In_2O_3 phase.[1] The Sn ESCA peaks from the as-grown surface had a composite structure (see Fig. 5). These Sn peaks are similar, in both shape and position, to those from the In_2O_3 powder mixed with 5 mol% SnO and 5 mol% SnO_2 (as shown in Fig. 3). Resolution of the Sn $3d_{3/2}$ peak into a SnO peak at 487.2 eV and a SnO_2 peak at 486.7 eV, as was done for the mixed powder, gave relative intensities corresponding to 60% SnO_2 and 40% SnO. ESCA results from the sanded surface, Fig. 5, also had a composite structure but shifted to lower binding energies by as much as 0.4 eV. In addition, the ratio of the Sn $3d_{3/2}$ to In $3d_{3/2}$ integrated areas changed from 0.051 before sanding to 0.035 after sanding, indicating a higher Sn content at the as-grown surface.

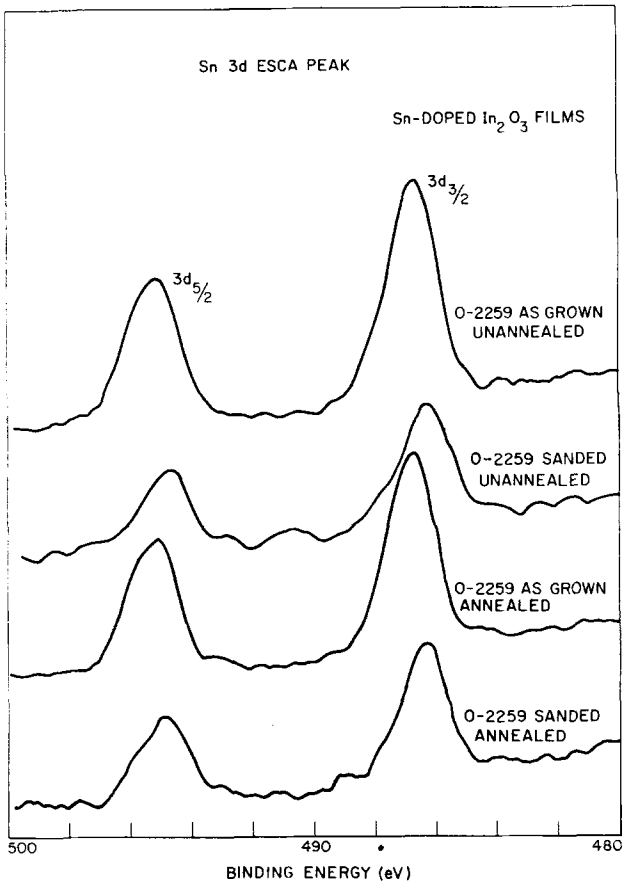

FIG. 6. Sn $3d_{3/2}$ and $3d_{5/2}$ ESCA peaks for an Sn-doped In_2O_3 film (0-2259) before and after annealing in O_2 at 500 °C.

The 600-W 0.6-μm-thick film 0-2259 was also clear; it had a visible transmission of over 85% and a room-temperature n-type resistivity $\rho \approx 2.6\times10^{-4}$ Ω cm. As shown in Fig. 6, the ESCA Sn peaks from the as-grown surface had a composite structure that could be resolved into SnO_2 and SnO $3d_{3/2}$ peaks at 486.7 and 487.2 eV with relative intensities of 80 and 20%. After sanding, the ESCA composite peaks were shifted about 0.4 eV toward lower energies and the Sn/In ratio decreased; the Sn $3d_{3/2}$ to In $3d_{3/2}$ ratio changed from 0.052 before sanding to 0.029 after sanding. As in film 0-2299, the Sn content appears to be significantly higher on the as-grown surface than in the bulk.

A second sample of the same 0-2259 film was annealed in O_2 at 500 °C for 4 h. The optical transmission was essentially unchanged, but the room-temperature resistivity increased to about 1×10^{-3} Ω cm. The ESCA Sn $3d_{3/2}$ peaks from the annealed surface were resolved into 486.7- and 487.2-eV peaks with intensities corresponding to 65% SnO_2 and 35% SnO. After sanding, the ESCA Sn peaks remained multiple but were shifted about 0.4 eV toward lower binding energies, as in the previous cases, and the ratio of Sn $3d_{3/2}$ to In $3d_{3/2}$ peak areas changed from 0.050 at the as-annealed surface to 0.028 at the sanded surface. In all our samples, we have observed no evidence of ESCA peaks from the metallic Sn.

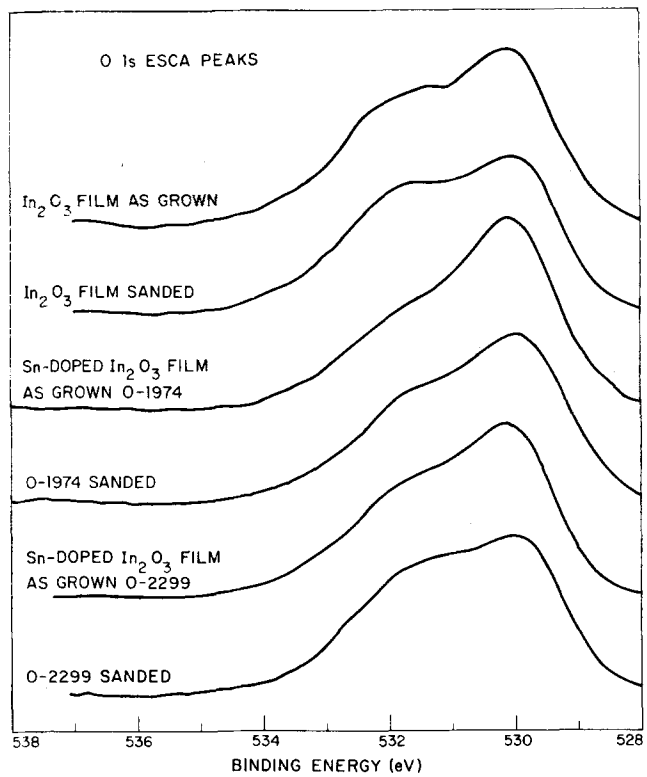

FIG. 7. O is ESCA peaks for an In_2O_3 film and several Sn-doped In_2O_3 films before and after sanding.

C. Oxygen 1s peaks

Figure 7 shows the oxygen 1s ESCA peaks observed from an In_2O_3 film and from the several Sn-doped In_2O_3 films discussed above. Since the results were similar for all the samples, we do not present all the data here. Table I summarizes the results.

TABLE I. Oxygen 1s peaks.

Samples	Positions (in eV) and relative strengths O_I	O_{II}	Area ratios $O_I+O_{II}/In\,3d_{3/2}$
In_2O_3 film	531.6	529.9	0.56
as-grown	52%	48%	
In_2O_3 film	531.6	529.9	0.56
Sanded	57%	43%	
0-1974	531.2	529.9	0.50
as-grown	47%	53%	
0-1974	531.3	529.8	0.55
Sanded	58%	42%	
0-2299	531.4	529.9	0.56
as-grown	52%	48%	
0.2299	531.3	529.8	0.58
Sanded	58%	42%	
0-2259	531.0	530.0	0.52
as-grown	50%	50%	
0-2259	531.2	529.8	0.56
Sanded	58%	42%	
0-2259 Ann.	531.4	530.0	0.55
as-grown	43%	57%	
0-2259 Ann.	531.2	529.9	0.57
Sanded	60%	40%	

1. In_2O_3

A 0.4-μm-thick In_2O_3 film (sputtered onto a Corning 7059 glass substrate from a 5-in-diam hot-pressed target of pure In_2O_3 at 550 W) had over 85% visible transmission and a room-temperature n-type resistivity $\rho \approx 7 \times 10^{-4}\ \Omega$ cm. The oxygen 1s ESCA peak from the as-grown surface had a composite structure that was resolved into two Gaussian peaks at 529.9 and 531.6 eV having relative peak-intensity ratios of 48 and 52%, respectively. The resolution procedure for the oxygen 1s peak used two Gaussian functions each of variable position, width, and intensity. Figure 8 shows the two resolved peaks. The relative O/In ratio was obtained by comparing the integrated areas of the oxygen 1s and In $3d_{3/2}$ peaks. This ratio is 0.56. After sanding, the oxygen 1s peak can again be resolved into 529.9- and 531.6-eV peaks but with relative intensities of 43 and 57% and the O/In ratio remained unchanged.

2. Sn-doped In_2O_3 films 0-1974, 0-2299, and 0-2259

For all the films, the oxygen 1s peaks were similar to that found for the In_2O_3 film. After sanding, the higher-energy component of the double peak always increased in relative intensity and the O/In ratio remained essentially unchanged. The higher-energy component is always much broader than the lower-energy one. However, annealing in O_2 appears to increase the relative intensity of the lower-energy component, as can be seen from Table I for the 0-2259 sample.

IV. DISCUSSION

In_2O_3 has the cubic bixbyite structure in which O^{2-} ions occupy, in an ordered manner, three-fourths of the tetrahedral interstices of a face-centered-cubic In^{3+}-ion array.[6] Indium oxide should have a filled $O^{2-}:2p$ valence band that is primarily oxygen 2p in character. The $In:3d^{10}$ core lies well below the valence-band edge E_v. Stoichiometric In_2O_3 would have an $In:5s$ conduction band with an edge E_c about 3.5 eV above E_v,[7] as shown in Fig. 9. The $O^{2-}:2p$ states are bonding; the $In:5s$ states are antibonding. As prepared, indium oxide is generally somewhat reduced; In_2O_{3-2x} corresponds to $InO_{(3/2)-x}\square_{(1/2)+x}$ where $\square$ symbolizes a vacant tetrahedral interstice of the face-centered-cubic In^{3+}-ion array. Of these vacancies, one-half per In^{3+} ion are ordered and x per In^{3+} ion are randomly distributed over the O^{2-}-ion subarray. These vacancies will be symbolized by V_0, signifying oxygen-array vacancies. Each V_0 is surrounded by In^{3+}-ion 5s orbitals that are stabilized from the $In:5s$ band by a lack of covalent bonding with the missing O^{2-} ion; therefore, symmetrized $In:5s$ orbitals at each V_0 form shallow donor states just below E_c that trap two electrons per oxygen vacancy. The measurements of Weiher[8] suggest a two-electron donor level about 0.03 eV below E_c for low x. At high V_0 concentrations (i.e., large x), a V_0 impurity band forms and overlaps E_c at the bottom of the conduction band, producing a degenerate semiconductor. This situation is shown schematically in Fig. 9. The density-of-states profile appears to have E_F below E_c for low V_0 concentrations, above it for higher V_0 concentrations. In order for reduced In_2O_3 films to remain clear while exhibiting a low resistivity, excitation of the mobile electrons to higher-lying 5s and 5p states must also require energies in excess of 3.5 eV.

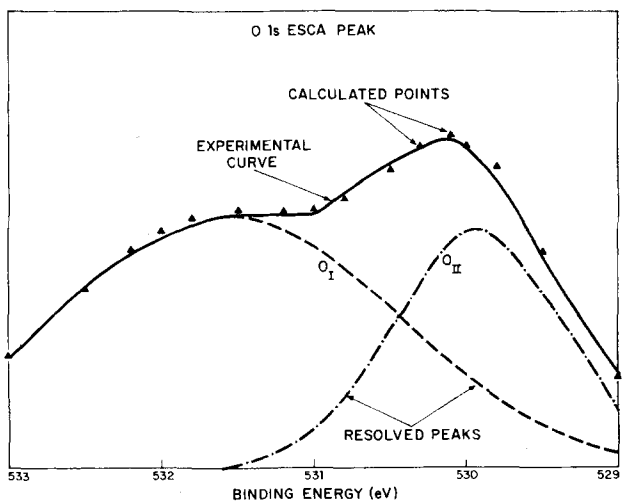

FIG. 8. O is ESCA peaks for the as-grown surface of an In_2O_3 film resolved into O_I and O_{II} peaks. The calculated points represent the superposition of the two resolved peaks.

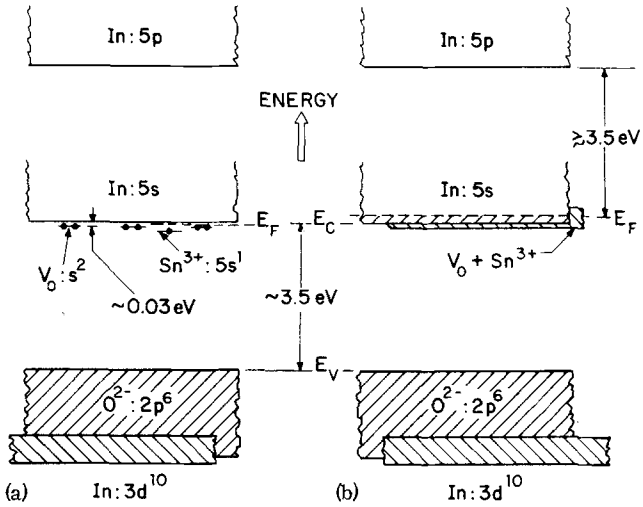

FIG. 9. Schematic energy-band model for Sn-doped In_2O_3, having no Sn_3O_4-like phase (a) for small x and (b) for large x.

In addition to providing conduction electrons, the x V_0's per In^{3+} also allow for O^{2-}-ion mobility. Therefore, In_2O_{3-2x} should be a mixed conductor, having both electronic and O^{2-}-ion conduction. The O^{2-}-ion conduction should be higher as x increases. Although the O^{2-}-ion conduction is insignificant compared to the electronic conduction, it may be critical for phase separation at relatively low temperatures.

Indium oxide may also be doped n type by the substitution of Sn for In. As for a conventional semiconductor, the donor atom has the larger nuclear charge, which stabilizes the $Sn:5s$ level just below E_c. Unlike the V_0 two-electron donor level, this is a one-electron level. In Sn-doped In_2O_3 films, V_0 and $Sn:5s$ donor levels should coexist and both should contribute conduction electrons (as shown in Fig. 9).

Sn-doped In_2O_3 films have traditionally been plagued with a darkening phenomenon; some films were dark either during preparation or after a period of time that varies with preparation conditions and ambience.[1,9] The ESCA data reported here, together with a reported mobile-electron concentration that is less than the total Sn concentration[1] for dark films, suggest that darkening is associated with the formation of a second phase in the bulk of the films. This possibility is a peculiar property of In^{2+} and Sn^{3+} ions, which tend to be stable only if isolated. Interactions between these cations in solids generally leads to an electron-transfer disproportionation,

$$2In^{2+} \rightarrow In^{+} + In^{3+},$$

$$2Sn^{3+} \rightarrow Sn^{2+} + Sn^{4+},$$

$$In^{2+} + Sn^{3+} \rightarrow In^{3+} + Sn^{2+}.$$

In the system under study, the number of mobile electrons in the In:5s conduction band appears too small for the disproportionation reaction $2In^{2+} \rightarrow In^{+} + In^{3+}$ to occur to any significant extent, and the ESCA peaks give no evidence of In^{+} or In^{2+} ions. In reduced In_2O_{3-2x}, the "extra" electrons tend to be trapped at the oxygen vacancies; in Sn-doped In_2O_3 some are trapped at Sn^{3+}-ion donor centers. Disproportionations that create Sn^{2+} ions induce local lattice relaxations that create longer Sn^{2+}-O^{2-} distances and shorter Sn^{4+}-O^{2-} distances. Shortened cation-anion distances and a higher formal valence state on the cation associated with the presence of Sn^{4+} ions enhance the covalent-mixing energy; this enhancement more than compensates for the increased electron-electron electrostatic energy due to placing two 5s electrons at an Sn^{2+} ion, especially if the local lattice strains are minimized by a cooperative formation of a second phase, Sn_3O_4. The structure of Sn_3O_4 is not well determined (most likely triclinic), but we may anticipate the formal valences $Sn_2^{2+}Sn^{4+}O_4$. Substitution of In for Sn in $Sn^{2+}_{2-y}Sn^{4+}_{1-y-2\varepsilon}In^{3+}_{2(y+\varepsilon)}O_{4-\varepsilon}$ could produce an oxygen-deficient phase having the structure of Sn_3O_4. Therefore, Sn-rich regions in reduced Sn-doped In_2O_{3-2x} can be expected to nucleate an Sn_3O_4-like phase. In addition, the enhanced O^{2-} ion mobility due to oxygen vacancies may induce the growth of such a phase at relatively low temperatures. (Similarly, a second phase containing spontaneously polarized In^{+} ions may be anticipated in very strongly reduced In_2O_{3-2x}, which is not the case in our films.)

In summary, Sn would normally enter the In_2O_3 lattice as an Sn^{3+} donor center. However, in the presence of oxygen vacancies, Sn-rich regions could nucleate an Sn_3O_4-like phase, darkening the Sn-doped In_2O_3 films and increasing the electrical resistivity. At high deposition temperatures and low deposition rates, the atomic mobilities are high enough relative to film growth for good homogenization of the films and for any second phase to be ejected to the surface. With lower deposition temperatures, the rate of film growth may be faster than the rate at which a second phase forms and migrates in the host structure. In the former case, films should exhibit an Sn-rich surface layer but remain clear; in the latter, the films would have an Sn-rich second phase dispersed through the bulk and be darkened. An aging phenomenon would be found where low ion mobilities slowed the nucleation and growth of the dispersed second phase.

These concepts permit a straightforward interpretation of the ESCA data presented as well as some interesting physical properties of this material system.

A. In $3d_{3/2}$ and $3d_{5/2}$ ESCA peaks

Since the extra electronic charge in In_2O_3 and Sn-doped In_2O_3 films is trapped only at V_0 and Sn centers, the In $3d_{3/2}$ and $3d_{5/2}$ peaks should be insensitive to the loss of oxygen and to the Sn concentration. This is consistent with our observation that In $3d_{3/2}$ and $3d_{5/2}$ peaks are essentially at the same location for all our samples.

B. Sn $3d_{3/2}$ and $3d_{5/2}$ ESCA peaks

The larger binding energy of the $3d^{10}$-core electrons in SnO versus SnO_2 reflects a smaller screening of these electrons from their nucleus. At a free atom, screening by the Sn $5s^2$ electrons should guarantee a smaller binding energy at Sn^{2+} versus Sn^{4+} ions. In a solid, on the other hand, covalent mixing can apparently reverse this order. Covalent mixing transfers charge from the anions back to the cations, thus enhancing the screening of the $3d^{10}$ electrons from the nuclear charge. The magnitude of this screening increases sensitively with the number of nearest-neighbor anions and decreasing cation-anion bond distance. In SnO_2, each cation with formal valence Sn^{4+} is surrounded by six nearest-neighbor O^{2-} ions at only 2.057 Å; in SnO, each Sn^{2+} cation has only four nearest-neighbor O^{2-} ions at 2.223 Å. Moreover, spontaneous polarization of the Sn^{2+} ion has displaced the lone-pair charge density to one side of the nucleus, thereby reducing the screening normally provided by a $5s^2$ core. Therefore, observation of a smaller binding energy for the Sn $3d^{10}$ core electrons in SnO_2 versus SnO can be understood.

Spontaneous cooperative polarization of Sn^{2+} ions commonly occurs in oxides rich in Sn^{2+} ions; 5s-5p hybridization displaces the center of electronic charge density to one side of the nucleus in order to permit stronger covalent bonding to anions on the opposite side. In SnO, the Sn-O distances indicate that the covalent bonding after polarization remains markedly less strong than that found in SnO_2. In Sn_3O_4 the Sn^{2+}-O^{2-} distances are presumably shorter, since the binding energies of the Sn^{2+} and Sn^{4+} ions are similar and about equal to those found in SnO_2.

The Sn-rich surface layer apparently represents a mixture of tin-oxide phases, In-substituted SnO, SnO_2, and/or Sn_3O_4. The 0.4-eV shift to lower binding energies for Sn $3d^{10}$ cores in the bulk of the Sn-doped In_2O_3 films may seem surprising in view of the apparently larger cation-anion separation of 2.18 Å.[1] (In_2O_3 without Sn doping has a separation of 2.167 Å.[10]) However, a substitutional Sn^{3+} ion donor center in the bulk has a different screening environment than the Sn^{2+} and Sn^{4+} ions at the surface. If there is no spontaneous displacement of the 5s charge density, screening of the $3d^{10}$-core electrons by the itinerant In 5s electron may be sufficient to account for the 0.4-eV shift.

C. Oxygen 1s ESCA peaks

The ESCA data distinguish two types of O^{2-} ions, O_I and O_{II}. The O_I : 1s peak has a binding energy about 1.5 eV higher than that of the O_{II} : 1s. Such a double oxygen 1s peak is common for oxides containing cations in multiple valence states.[11] These data suggest that the O_{II}^{2-} ions have neighboring In atoms with their full complement of six nearest-neighbor O^{2-} ions, that the O_I^{2-} ions are in oxygen-deficient regions. Since the In $3d_{3/2}$ and $3d_{5/2}$ ESCA peaks are insensitive to the loss of oxygen, we may conclude that the charge density at the In^{3+} ions is not significantly changed even though the V_0-trap orbitals are formed from symmetrized 5s wave functions of the neighboring In atoms. The anion subarray plus the oxygen vacancies V_0, therefore, must also carry the same net electronic charge with and without the vacancies. However, the presence of anion vacancies changes the distribution of the negative-charge density. An electron charge density in the region of a V_0 reduces, at the nearest-neighbor O^{2-} ions, the screening of the O^{2-} : 1s electrons from their nucleus, thus raising the effective nuclear charge Z_{eff} (i.e., the binding energy) of an O_I^{2-} : 1s electron relative to that of an O_{II}^{2-} : 1s electron. The magnitude of the shift to higher binding energies should vary with the oxygen deficiency associated with the nearest-neighbor In^{3+} ions, so that the O_I^{2-} : 1s peak is broadened and its amplitude increases with the V_0 concentration x. The relative shift is not altered by the presence of itinerant 5s electrons, which are shared equally by all the In atoms. In air, the surfaces of the Sn-doped In_2O_3 films tend to be richer in oxygen than the bulk, and from the above interpretation, the O_{II} peak should have a higher relative intensity at the surface than in the bulk. This is indeed the case, as shown in Table I. Similarly, the O_{II} peak of sample O-2259 has a higher relative intensity after annealing in oxygen than before, consistent with the model. The oxygen 1s ESCA peak for In_2O_3 powder also shows the presence of a weak O_I^{2-} peak, with a relative peak strength of about 30%. This suggests that the In_2O_3 powder is already slightly reduced and explains why the powder is sufficiently conducting that no charging effects were observed in our experiments.

D. Electrical resistivity

From the band model of Fig. 9, the resistivity ρ of $In_{2-\alpha}Sn_\alpha O_{3-2x}$ is dominated by itinerant electrons in the conduction band. Therefore, if n is the effective density of itinerant electrons having a mobility μ, the resistivity follows the simple equation $\rho \approx (ne\mu)^{-1}$. For $\alpha = 0$ and small x, the Fermi energy E_F may fall below the conduction band edge E_c; but, in general, $n \approx \alpha + x$ and the films are degenerate semiconductors. The decrease in mobility μ with increasing $\alpha + x$ (due to impurity scattering) is compensated by the increase with $\alpha + x$ in the number of mobile charge carriers. The above discussion is consistent with the observed results. For In_2O_3 crystals with very little oxygen deficiency $\mu_H \approx 160$ cm^2/V sec and $n \cong 10^{18}$/cm^3.[8] In our In_2O_3 films $\rho \approx 7 \times 10^{-4}$ Ω cm, $\mu_H \approx 90$ cm^2/V sec, and $n \cong 10^{20}$/cm^3; in Sn-doped In_2O_3 films $\rho \approx 2 \times 10^{-4}$ Ω cm, $\mu_H \approx 40$ cm^2/V sec, and $n \cong 8 \times 10^{20}$/cm^3. Our observed increase in ρ after annealing in oxygen, which decreases x, is also compatible with this model.

E. Absorption-band edge

An optical absorption band sets in for photon energies larger than that required to excite an electron from the valence band to the conduction band. For a degenerate semiconductor, the excitation energy is $E_g(\text{eff}) = E_F - E_v = \Delta E + E_c - E_v$, where ΔE accounts for the shift in E_F as n changes. Thus, $E_g(\text{eff})$ increases with n even if $E_v - E_c$ remains essentially constant (Burstein effect[12]), and such a dependence in Sn-doped In_2O_3 has been reported.[7] This argument requires that the optical transitions from E_F to higher bands are at an energy larger than $E_g(\text{eff})$. In other words, E_F would appear to be between widely separated In^{3+} : 5p and O^{2-} : 2p bands having a minimum separation of about 7 eV (as shown in Fig. 9).

F. Film darkening

According to the model, film darkening is due to trapping of an Sn_3O_4-like phase in the bulk. At the surface, Sn_3O_4 probably decomposes to $2SnO + SnO_2$ (as suggested by our ESCA results). Thermodynamics apparently favors migration of the Sn-rich phases to the surface, and a distinguishable surface layer is only found at the surface if the substrate temperature is high enough relative to the deposition rate to permit equilibrium to be established. The existence of an Sn-rich surface layer is apparent in our ESCA results, and such a surface layer has also previously been suggested based on the infrared reflectivity data on Sn-doped In_2O_3 films.[13] The 100-W film 0-1974 is not at equilibrium, containing some trapped second phase in the bulk, and an Sn-rich surface layer is absent. Aging that produces a sudden darkening of the film is probably caused by diffusion-induced formation and/or growth of a second phase trapped in the bulk. The film would be darkened to varying degrees, depending on the second phase present in the bulk. Stable Sn-doped In_2O_3 films can be prepared by raising the substrate temperature sufficiently to allow equilibrium to be established. According to this model, there should be an optimal Sn doping in In_2O_3 for the maximum conductivity. A further increase in Sn-doping will either induce the Sn_3O_4-like phase or just accumulate as Sn^{2+} and Sn^{4+} on the surface, resulting in no increase, or even a decrease, in conductivity. Such a conductivity dependence on the Sn-doping level has been reported.[2] We also anticipate that deposition in a higher oxygen partial pressure should suppress the formation of oxygen vacancies, thus lowering the probability of nucleating an Sn_3O_4-type second phase. In this case, lower substrate temperatures should be tolerable.

G. Oxidation

As stated earlier, x oxygen vacancies per molecule in the Sn-doped In_2O_3 films allow O^{2-}-ion conduction; conduction increases as x increases. During postdeposition annealing, x rapidly vanishes in the surface layer and oxygen-ion conduction decreases (or even ceases), terminating further oxidation into the bulk. Such an oxidation-limiting process has been reported,[14] and this effect could explain the long-term stability of properly prepared films. Our films prepared at high substrate temperatures have been stable for at least two years.

ACKNOWLEDGMENTS

The authors acknowledge Paul E. Larson for operating the ESCA apparatus and for many helpful discussions. The technical assistance of George H. Foley and Paul M. Zavracky is greatly appreciated.

The views and conclusions contained in this paper are those of the contractor and should not be interpreted as necessarily representing the official policies, either expressed or implied, of the United States Government.

[1]J.C.C. Fan and F.J. Bachner, J. Electrochem. Soc. **122**, 1719 (1975).
[2]D.B. Fraser and H.D. Cook, J. Electrochem. Soc. **119**, 1368 (1972).
[3]J.C.C. Fan and F.J. Bachner, Appl. Opt. **15**, 1012 (1976).
[4]J.R. Bosnell and R. Waghorne, Thin Solid Films **15**, 141 (1973).
[5]W.E. Morgan and J.R.V. Wazer, J. Phys. Chem. **77**, 965 (1973).
[6]R.W.G. Wyckoff, *Crystal Structures*, 2nd ed. (Wiley, New York, 1964), Vol. 2, p. 2.
[7]V.M. Vainshtein and V.I. Fistul, Sov. Phys.-Semicond. **1**, 104 (1967); H.K. Müller, Phys. Status Solidi **27**, 723 (1968).
[8]R.L. Weiher, J. Appl. Phys. **33**, 2834 (1962).
[9]J.L. Vossen and E.S. Poliniak, Thin Solid Films **13**, 281 (1972).
[10]Reference 6, pp. 136 and 250.
[11]J.P. Bonnelle, J. Grimblot, and A. D'Huysser, J. Electron Spectrosc. Relat. Phenom. **1**, 151 (1975).
[12]E. Burstein, Phys. Rev. **93**, 632 (1954).
[13]V.M. Vainshtein and V.I. Fistul, Sov. Phys.-Semicond. **4**, 1278 (1971).
[14]S. Sobagina, H. Okaniwa, N. Takogi, I. Sugiyama, and K. Chiba, Jpn. J. Appl. Phys. (Suppl) **2**, 475 (1974); (private communications).